Stress-based model on work hardening and softening of materials at large strains: corrugation process of sheet

E. Hosseini · M. Kazeminezhad

Abstract In this article, a stress-based model is proposed to investigate the strength evolution during severe plastic deformation (SPD) or large strains. In this model, the work hardening mechanisms are described by Frank-Read sources, while the cross-slip and climb processes are considered as the mechanisms for work softening phenomenon. Within all SPD processes, one of corrugation processes such as constrained groove pressing is chosen to assess the validity of the model predictions. The model predictions are in agreement with the earlier reports and the experimental results achieved in this study.

Introduction

The prediction of material properties with the aid of computer simulations offers low time prototyping and low cost process development in industrial processes [1–3]. Thus, numerical simulations are nowadays commonly used in industry for the setting of the forming technologies concerning new parts products, and several commercial computer codes are available for this purpose [4]. During the past few years, intensive works have been carried out to obtain the most reliable numerical tools for improving simulations of sheet metal forming operations [4] and hence, finite-element method (FEM) has become a very useful tool for engineers and scientists [1]. However, the theory of FEM is based on constitutive equations and usually isotropic or perfectly plastic relations are considered as constitutive

E. Hosseini · M. Kazeminezhad (✉)
Department of Materials Science and Engineering, Sharif University of Technology, Azadi Ave., Tehran, Iran
e-mail: mkazemi@sharif.edu

equations in FEM simulations [1]. Using this assumption, it is not possible to make predictions with sufficient accuracy [1], because strain hardening is an important parameter that describes the plastic behavior of polycrystalline materials and it can strongly affect plastic flow localization, fracture, and other phenomena that involve plastic deformation [5]. Also, in some developed commercial FEM codes, simple empirical work hardening descriptions are used, which often give a remarkably good fit to the measured data [6], but as well as these empirical relations are usually compatible for small magnitude of deformations, this consideration does not allow any extrapolation beyond the range of experimentally examined deformation conditions [1, 7]. The best way to reform the FEM simulations to be applicable for wide range of conditions is linking this approach by the work hardening models based on physical assumptions, which were derived by theory and proved by experiments [1]. Thus, it is mandatory to use true internal state variables of the material to present the flow behavior of materials for a wide range of strains, strain rates, temperatures, and material chemistry [8]. Within the proposed internal state variables, dislocations are important factors in controlling the mechanical properties and there have been numerous attempts with limited success in the past to model the flow behavior of materials based on dislocation concepts [6–8]. It should be noted that in general, a proper model should be able to predict the flow behavior of materials in terms of internal variables, based on the special physical mechanisms [9]. However as cited in following, most of presented models considered some pure mathematical terms that do not related to specific mechanism in materials [6, 10] and it seems that more scientific work is required.

In order to model the wok hardening and softening, in primary attempts, the overall dislocation density was used (one-parameter models) as internal variable [11]. But, an

application to a wide range of strains, strain rates, and temperatures turned out to be difficult with a single material parameter [7]. Many investigations in the last two decades clearly showed the occurrence of two new universal hardening stages (IV, V) for both low and high deformation temperatures [12]. While the first exhibits a steady hardening behavior similar to stage II, the second approaches and includes a steady-state deformation where both the flow stress as well as the dislocation density remains constant [10]. However, it has been shown by several theoretical treatises that these models fail in describing these two stages [12].

Two separate dislocation densities models (two-parameter models) were commended after one-parameter models [13, 14]. Rather, from the heterogeneous character of microstructure, which typically develops at strains larger than true strain $\varepsilon = 0.1$ [12], it can be ascertained the material can be treated as a two-phase composites consisting of cell walls of high dislocation density and cell interiors with relatively low dislocation density [10, 15]. Thus in these models, the dislocation densities in cell interiors and cell walls are treated separately [7, 10]. In the models, simple physical descriptions are used for increasing of the dislocation densities [16]; however, for decreasing of the dislocation densities no special physical consideration is considered and thus the later phenomenon appears in form of mathematical constants [17]. Although these models often give a remarkably good fit to experimental data for large broad of strain and strain rate [16], the mathematically determined constants cannot be usable for conditions where the temperature and material type are changed [1, 7]. In other words, since the determined constants are not based on the physical or metallurgical concepts and just achieved on the basis of mathematical fitting, they are not reliable to be used for the other conditions. However, as these models are the unique ones that can investigate the flow behavior of materials through large strains, it seems that more investigations, especially on the decreasing of the dislocation densities, are required to study the flow behavior of material in large deformation for larger broad of temperatures and material chemistries.

Three separate dislocation densities are distinguished in three-parameter models [6]. The third internal variable is the density of mobile dislocations, which carry the plastic strain [7]. Although these models can investigate the flow behavior of materials by completely physical considerations [18], they cannot consider screw dislocations and hence are only valid for high-temperature deformation [6]. It is worth to note that no attempt is carried out to examine these models for large deformations at neither low temperatures nor high temperatures. Because in high degree of strains the role of screw dislocations becomes more important.

Here, considering the dislocation densities evolutions, a stress-based model is proposed that based on thoroughly physical concepts, which considers the effects of stress field in materials on dislocation interactions and the parameters such as material chemistry, temperature, etc. This approach, which is simple in its mathematical form and, notably, contains a relatively small number of adjustable material parameters, treats flow hardening in materials process to high degree of strains.

Severe plastic deformation (SPD) is one of the most common methods for introducing large magnitude of deformation [19–26]. The SPD processes are frequently used for producing ultrafine-grained materials with high strength and acceptable ductility [14, 20, 21, 27, 28]. SPD processes are involved different methods such as equal channel angular pressing [29–32], high-pressure torsion (HPT) [14, 33], accumulative roll bonding (ARB) [34, 35], repetitive corrugation and straightening (RCS) [27], constrained groove rolling (CGR) [36], constrained groove pressing (CGP) [37], and so on. Within these methods, the first two methods are related to bulk deformation process and have investigated in previous works by both mechanical and metallurgical models [13, 14, 16, 30, 38]. However, a limited metallurgical modeling works have been carried out on the processes related to the SPD of sheets. Considering the last four processes that are applicable to sheets, ARB involves repetitive bonding between two rolled plates, which may cause imperfect bonding in the material, leading to the reduction of product mechanical properties [24]. Thus, the ARB is less considered feasible for SPD of sheet metals. The RCS process that is consist of unconstrained corrugation and straightening introduces some elongation to the specimen [27], causing strain inhomogeneity in the sheets. In the CGR process, deformation is applied by rolling mechanism [36], which may create additional tensile strain in the specimen due to bending strain condition, leading to crack nucleation and growth. In the CGP, the strain is imposed by means of non-round die in a constrained condition; therefore, no significant strain inhomogeneity or bending strain occurs [24], and in this study the inhomogeneity is ignored.

The principle of CGP is subjecting a sheet to a large amount of plastic shear deformation with asymmetrically grooved and flat dies pressing, alternatively [39]. The gap between the upper die and the lower die is the same as the sample thickness, and mechanical analysis shows that deformation occurs in plane strain pure shear condition [39]. Therefore, in this article the CGP process is chosen to investigate the validity of stress-based model. The studied material is commercially pure copper. Therefore, the process is performed experimentally and the achieved results are compared with the modeling results at different passes.

Stress-based model

Concept

The model proposed in this article can be applied to pure materials that, with progressing the strain, a cell structure develops consisting of cell walls of high strength and cell interiors of low strength. For investigating the strength evolution, dislocation reactions in both phases and their effects on strength of cell interiors and cell walls and over all strength are regarded. Increasing in the strength is related to increasing the dislocation densities due to Frank-Read source, and decreasing mechanism of strength is dynamic recovery. In addition, the effect of dislocation transition from cell interiors to cell walls and also the effects of stress field in cell interiors on the strength evolution are considered. Moreover, it is assumed that the major relaxation of material in cell interiors and cell walls are related to annihilation of screw dislocations and edge dislocations, respectively [40–42]. Here, polycrystal behavior is introduced by the average Taylor factor (M) [7].

The model

Considering the material as two phases composite and the mixture rule, the following relation can be written [16]:

$$\sigma = f\sigma^{w} + (1-f)\sigma^{c}, \tag{1}$$

where σ, σ^{c}, σ^{w} are strengths of over all, cell interiors, and cell walls, respectively, and parameter f defines the volume fraction of cell walls. The cell walls volume fraction varies with the accumulation of strain and has been shown to either decrease with strain monotonically to a saturated value [11, 43], or first increase with accumulated strain and then decrease with strain monotonically [30]. From the experimental data on copper, the variation of the volume fraction of the walls with the shear strain is estimated by the following relationship [10]:

$$f = f_{sat} + (f_{ini} - f_{sat})\exp\left(-\frac{\varepsilon}{\eta_{1}}\right), \tag{2}$$

where f_{ini} is the initial volume fraction, f_{sat} is the saturated value, ε is the shear strain, and η_{1} is a numerical constant. The strength in each phase is consisted of two sections:

$$\sigma^{i} = \sigma_{thermal}^{i} + \sigma_{athermal}^{i}, i = w, c, \tag{3}$$

where $\sigma_{thermal}^{i}$ is the stress related to lattice friction and solute content that considered to be temperature dependent, and $\sigma_{athermal}^{i}$ is the stress mainly related to dislocation interaction through [44]:

$$\sigma_{athermal}^{i} \propto \frac{1}{\Lambda^{i}}, i = w, c, \tag{4}$$

where Λ^{i} is the average distance between dislocations in each phase and is inversely proportional to the square root of dislocation density in that phase. Therefore, it can be assumed:

$$\begin{aligned}\sigma &= \sigma_{thermal} + \sigma_{athermal} \\ &= \sigma_{thermal} + \left(f\sigma_{athermal}^{w} + (1-f)\sigma_{athermal}^{c}\right).\end{aligned} \tag{5}$$

Hence, considering the strength evolutions in the phases, it is possible to study the over all strength variation through straining.

Athermal strength evolution in the cell interiors can be defined as:

$$\frac{d\sigma_{athermal}^{c}}{dt} = \left(\frac{d\sigma_{athermal}^{c}}{dt}\right)^{+} + \left(\frac{d\sigma_{athermal}^{c}}{dt}\right)^{-}, \tag{6}$$

where the first term represents the work hardening phenomenon and the second one represents the work softening phenomenon. Regarding the dislocation interactions [10] in the cell interiors, the above-mentioned equation can be described as:

$$\begin{aligned}\frac{d\sigma_{athermal}^{c}}{dt} = &\left(\frac{P_{1}\alpha\mu M^{2}}{2\sqrt{3}} \cdot \frac{\sigma_{athermal}^{w}}{\sigma_{athermal}^{c}}\dot{\varepsilon}\right) \\ &- \left(\frac{3P_{2}\alpha^{2}\mu^{2}M^{3}b}{K} \cdot \frac{\sigma_{athermal}}{(1-f)^{1/3}\sigma_{athermal}^{c}}\dot{\varepsilon}\right) \\ &- \left(\frac{C_{1}v_{0}\mu M^{2}}{2w} \cdot \left[\exp\left(-\frac{Q_{cs}}{K_{b}T}\left(1 - \frac{\sigma_{athermal}^{c}}{M\mu}\right)\right)\right.\right. \\ &\left.\left. - \exp\left(-\frac{Q_{cs}}{K_{b}T}\right)\right]\right), \tag{7}\end{aligned}$$

where P_{1}, P_{2} are the probability constants that are identified in Refs [13, 16], μ, b, $\dot{\varepsilon}$, and T are the shear modulus, the magnitude of Burgers vector, the strain rate, and the absolute temperature, respectively. Also, v_{0} and w are the frequency of annihilation attempts and length of a potential site for annihilation of screw dislocations and, Q_{cs} and K_{b} are the activation enthalpy of cross-slip and Boltzmann's constant, respectively. The parameter C_{1} is a numerical constant and K defines as:

$$K = \sigma_{athermal} \cdot d, \tag{8}$$

where d is the cell size. Prior works showed that K is a function of strain through [14, 45]:

$$K = K_{sat} + (K_{ini} - K_{sat})\exp(-\eta_{2}\varepsilon), \tag{9}$$

where K_{ini} is the initially value of K, and K_{sat} is the saturated value of K. Also, η_{2} is a numerical constant.

The three terms on the right-hand side of Eq. 7 are the contributions from different mechanisms. The first one is related to the effect of dislocation generation due to Frank-Read sources at the interface of cells. The second term describes the softening in cell interiors caused by the dislocation transition from the cell interiors to the cell walls, and the last term describes dynamic recovery in cell interiors that assumed to occur through cross-slip of screw dislocations [16]. Third term shows that increasing the stress field in cell interiors causes accelerating the kinetics of softening.

In similar way, athermal strength evolution in the cell walls can be defined as:

$$\frac{d\sigma_{athermal}^{w}}{dt} = \left(\frac{d\sigma_{athermal}^{w}}{dt}\right)^{+} + \left(\frac{d\sigma_{athermal}^{w}}{dt}\right)^{-}, \tag{10}$$

$$\begin{aligned}\frac{d\sigma_{athermal}^{w}}{dt} &= \left(\frac{3P_2\alpha^2\mu^2 M^3 b}{K} \cdot \frac{(1-f)^{2/3}\sigma_{athermal}}{f\sigma_{athermal}^{w}}\dot{\varepsilon}\right) \\ &\quad + \left(\frac{\sqrt{3}P_2\alpha\mu M^2}{2} \cdot \frac{(1-f)}{f}\dot{\varepsilon}\right) \\ &\quad - \left(\frac{C_2 b D_L}{2K_b T\mu\alpha^2 M^2} \cdot \left(\sigma_{athermal}^{w}\right)^3\right), \end{aligned} \tag{11}$$

where D_L is the lattice diffusivity and C_2 is a numerical constant.

The first term on the right-hand side of Eq. 11 represents the effect of the dislocation flux coming from the cell interiors, second term is related to the effect of Frank-Read activity in cell walls interfaces, and the last term describes dynamic recovery in cell walls that assumed to occur through climb of edge dislocations [16].

Solving these equations with proper initial conditions can predict the evolution of strength during forming process. It should be noted that this model is physical base and has a low number of mathematical constants in comparison with other similar mentioned-models.

Modeling procedure

In order to assess the validity of the model, it is applied on the CGP process of copper sheets. Considering the presented model, the set of differential equations can be solved for a defined strain rate field.

Mechanical analysis shows that the shear-strain rate in each stage can be calculated through the following equation (see Fig. 1):

$$\dot{\varepsilon}_{xy} = \dot{\varepsilon}_{yx} = \frac{1}{2}\left(\frac{\partial \dot{U}_x}{\partial y} + \frac{\partial \dot{U}_y}{\partial x}\right) = \frac{1}{2}\frac{d\dot{U}_y}{dx} \approx \frac{1}{2}\frac{V_0}{t_0}, \tag{12}$$

where, $\dot{U}_x$ and $\dot{U}_y$ are the velocity vectors in x and y directions, respectively, V_0 is the crosshead speed, and t_0 is

the sheet thickness. Then, considering the CGP process as a plane strain process, the Von-Mises strain rate can be computed by:

$$\bar{\dot{\varepsilon}}_{Mises} \approx \frac{1}{\sqrt{3}}\frac{V_0}{t_0}. \tag{13}$$

All of the model parameters and constants used in the present model are summarized in Table 1. The mentioned set of differential equations is solved numerically by finite difference method and the outcomes are presented in "Results and discussion" section.

Experimental material and procedures

The material used in this study was commercial purity (99.5%) copper sheets. The dimension of the CGP samples was $90 \times 60 \times 3$ mm^3. Before CGP, all samples were annealed at 1023 K for 3 h and then the samples were processed at room temperature from one to three passes. Each pass of this process was consisted of four stages and the process was carried out by two pair of dies. The schematic of corrugating die and flattening die are presented in Fig. 1a and b. At first stage, the flat copper sheet (Fig. 1c) became corrugated (Fig. 1d) by the corrugating die and then the flattening die flattened the corrugated sheet (Fig. 1e). It is worth to note in this stage, the sheet was consisted of two sections with 0 and 1.15 strains. In order to homogenize the magnitude of strain, the sheet was rotated for 180° around it normal axis and then the above stages were repeated (Fig. 1f, g). Therefore, at the end of fourth stage, the sheet has a uniform strain magnitude of 1.15. The practically processed sample of Fig. 1f can be observed in Fig. 1h.
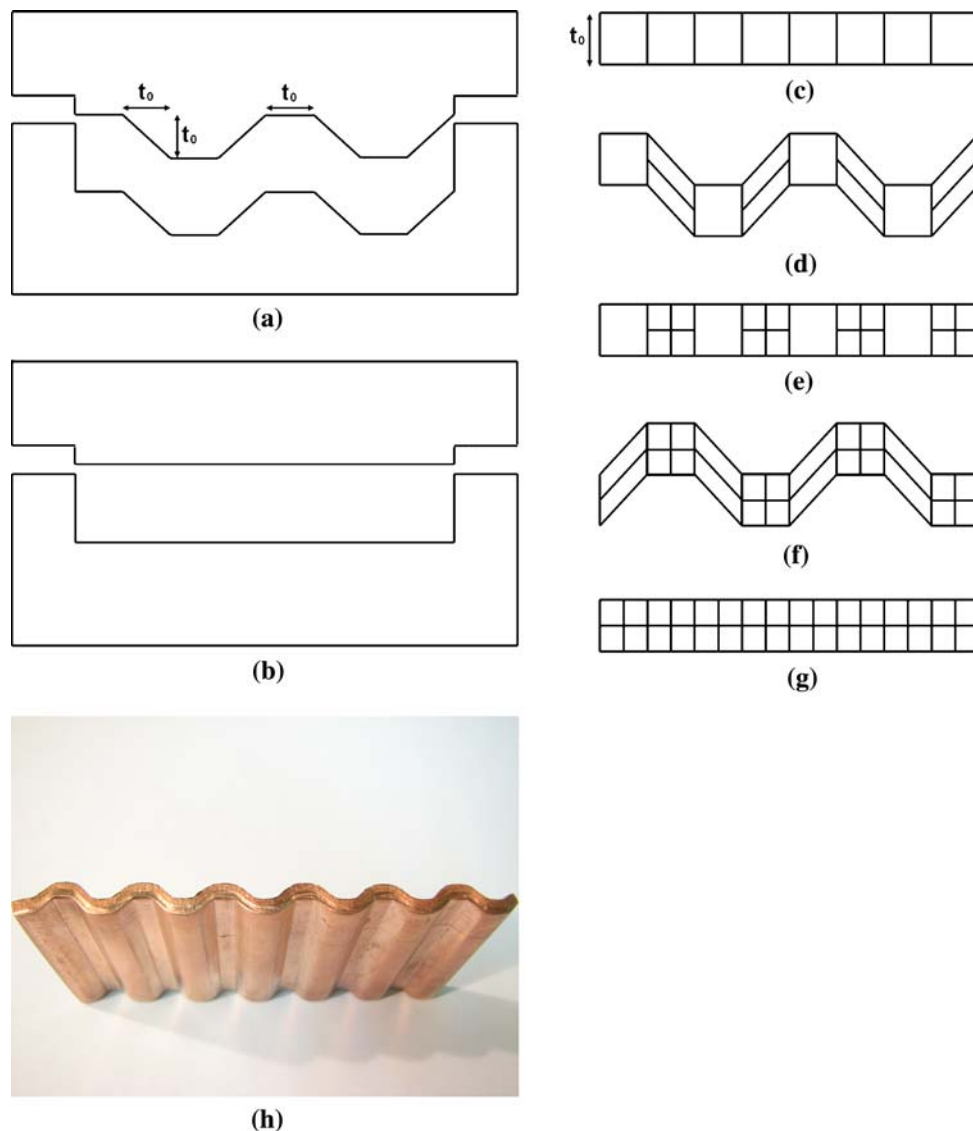
All of the passes were carried out using a pressing machine with a ram speed of 0.15 mm s^{-1}. According ASTM E8M standard tensile tests were performed on the specimens with gage length of 32 mm, width of 6 mm, and thickness of 3 mm using a tensile testing machine at a crosshead speed of 0.15 mm s^{-1}.

Results and discussion

From the above-mentioned model, the athermal strengths within the cell interiors, $\sigma_{athermal}^{c}$, and cell walls, $\sigma_{athermal}^{w}$, are calculated and presented in Figs. 2 and 3.

Through the first CGP pass, the model predicts a rapid increase in the athermal strength of both cell interiors and cell walls from the initial magnitudes to the magnitudes of 105 and 520 MPa, respectively. In following passes, the athermal strength of the cell walls is increased continuously with low rate and reaches to 610 MPa at the end of

pressing (Fig. 2). This prediction shows that the work hardening mechanisms in the cell walls are predominant in comparison with work softening mechanisms through all passes. An analogues trend was predicted for dislocation density in cell walls for Al by McKenzie et al. [16] and also reported in some earlier experimental studies [14] on other SPD processes.

As it can be seen in Fig. 3, the athermal strength of cell interiors reaches to a saturation magnitude, and then a little drop is predicted at last passes. This dropping in the athermal strength of cell interiors shows that work softening is predominant after first pass. Work softening mechanisms in the cell interiors after first pass are a transformation stage of cells that cause to formation of cells with low dislocation density, as well as dynamic recovery. Evidence of occurring this transformation reported through TEM observation by Krishnaiah et al. [39] worked on Al processed by CGP. In

addition, this is confirmed by the measurements of dislocation density carried out for severely deformed copper in HPT [14]. It is interesting to note that this phenomenon was predicted in only some versions of two internal variables models that applied on SPD process [14, 45] and in most of them that assumed an inversely linear relation between cell size and square root of dislocation density [16], this phenomenon was unpredictable.

However, as can be seen in Fig. 4 the overall strength through tensile test is increased rapidly to a value of 215 MPa in first pass and then it reaches to a saturation value with small drop at the end of process. These results show that through deformation before first pass, work softening mechanisms cannot soften the material; however after first pass, the softening mechanisms are predominant and the material is softened. The validity of the predicted results is checked by the experimental strength and as

Brief description of parameter	Abbreviation	Value
Probability constant of cell interiors	P_1	0.0024
Probability constant of cell walls	P_2	0.0054
Magnitude of the Burgers vector for Cu (m)	b	2.56×10^{-10}
Initial cell interiors strength (MPa)	$\sigma^c_{athermal,t=0}$	36.9
Initial cell walls strength (MPa)	$\sigma^w_{athermal,t=0}$	82.5
Constant in the dynamic recovery term for cell interiors	C_1	1×10^{16}
Constant in the dynamic recovery term for cell walls	C_2	1×10^{19}
Initial value of cell walls volume fraction	f_{ini}	0.25
Saturated value of cell walls volume fraction	f_{sat}	0.07
Numerical constant	η_1	3.2
Initial value of K (MN m^{-1})	K_{ini}	115.43
Saturated value of K (MN m^{-1})	K_{sat}	49.46
Numerical constant	η_2	0.79
Taylor factor	M	3.06
Weight of the dislocation interactions	α	0.25
Shear modulus (GPa)	μ	42.1
Lattice friction stress (MPa)	$\sigma_{thermal}$	25
Boltzmann's constant (J K^{-1})	K_b	1.38×10^{-23}
Activation enthalpy of cross-slip (J)	Q_{cs}	6.24×10^{-19}
Lattice diffusivity (m^2 s^{-1})	D_L	3.33×10^{-38}
Frequency of annihilation attempts (s^{-1})	v_0	1×10^9
Length of a potential site for annihilation of screw dislocations (m)	w	$1000b$

Table 1 The values of parameters and constants used in the model [10, 13, 14, 16, 38, 45, 47–49]
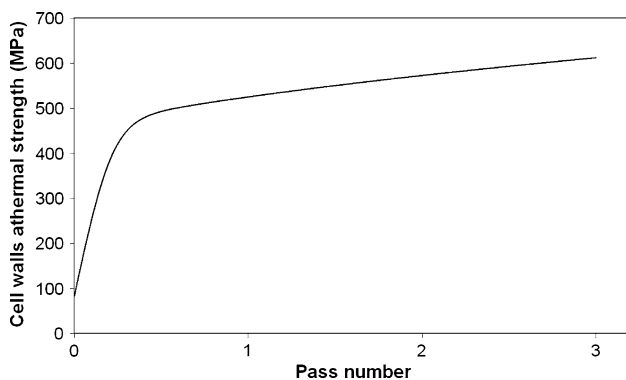

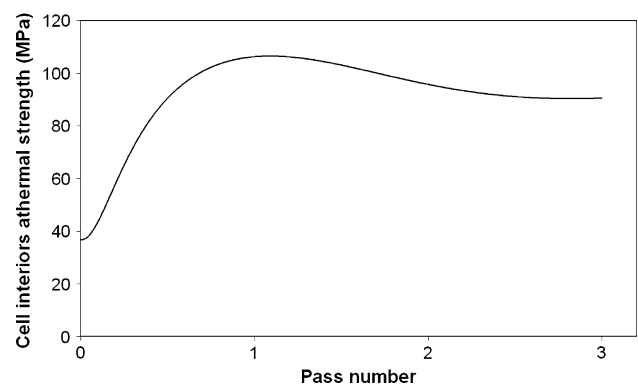**Fig. 2** The athermal strength in the cell walls versus pass number

Fig. 3 The athermal strength in the cell interiors versus pass number

can bee seen, a remarkable agreement between them is obtained. It should be noted that the magnitudes of the strength illustrated in Fig. 4 are in agreement with the reported data on CGP process of copper sheets by Krishnaiah et al. [39].

By comparing the strengths of copper processed by CGP with that processed by the other SPD processes [3, 23], it can be found that the strength of copper processed by CGP is lower. This difference mainly arises from the difference between the deformation paths of the processes. Also, it should be considered that for the sheet metals, free surface to volume ratio is larger than that of bulk materials and since free surface can act as dislocation annihilator [46], so

it is reasonable to observe higher dislocation annihilation in sheets. Considering these topics, it is logical to observe lower strength in copper sheets processed by CGP.

Conclusions

In this study, considering the dislocation evolution mechanisms, a stress-based model is proposed to investigate the evolution of the strength during large deformation magnitude. The process of CGP is chosen as an experimental process to introduce a large magnitude of deformation. The model predicts that the strength is increased in both cell
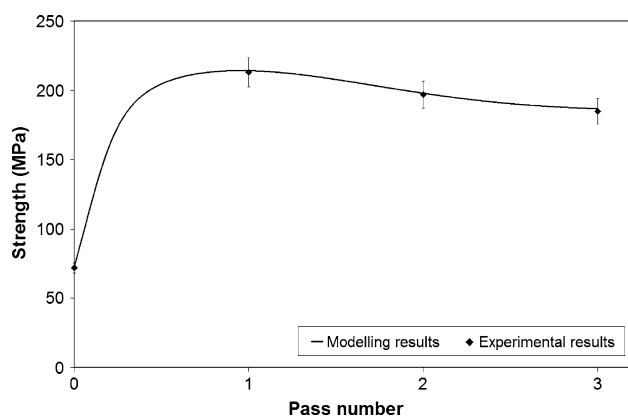
Fig. 4 The overall strength versus pass number

interiors and cell walls through first pass. Then the strength in the cell walls is increased continuously, but the strength in cell interiors shows a little drop.

In addition, the model predicts a drop in the overall strength after a rapid increase in first pass. This trend describes a competition between work hardening and work softening mechanisms. During first pressing, the work hardening mechanisms are predominant; however, in following passes the work softening mechanisms are predominant. Also, the results obtained by the experiment show a remarkable good agreement with the modeling results.

References

1. Aretz H, Luce R, Wolske M et al (2000) Modell Simul Mater Sci Eng 8:881
2. Estrin Y, Kim HS (2007) J Mater Sci 42:1512. doi:10.1007/s10853-006-1282-2
3. Kazeminezhad M, Hosseini E (2008) J Mater Sci 43:6081. doi:10.1007/s10853-008-2953-y
4. Haddadi H, Bouvier S, Banu M et al (2006) Int J Plast 22:2226
5. Lopesa AB, Barlatb F, Gracioc JJ et al (2003) Int J Plast 19:1
6. Roters F, Raabe D, Gottstin G (2000) Acta Mater 48:4181
7. Goerdeler M, Crumbach M, Schneider M et al (2004) Mater Sci Eng A 387–389:266
8. Prasad GVSS, Goerdeler M, Gottstein G (2005) Mater Sci Eng A 400–401:231
9. Ma A, Roters F (2004) Acta Mater 52:3603
10. Estrin Y, Toth LS, Molinari A et al (1998) Acta Mater 46:5509
11. Estrin Y, Mecking H (1984) Acta Mater 32:57
12. Mulders B, Zehetbauer M, Gottstein G et al (2002) Mater Sci Eng A 324:244
13. Baik SC, Estrin Y, Kim HS et al (2003) Mater Sci Eng A 351:86
14. Estrin Y, Molotnikov A, Davies CHJ et al (2008) J Mech Phys Solids 56:1186
15. Richert M, Stuwe HP, Zehetbauer MJ et al (2003) Mater Sci Eng A 355:180
16. Mckenzie PWJ, Lapovok R, Estrin Y (2007) Acta Mater 55:2985
17. Toth LS, Molinari A, Estrin Y (2002) J Eng Mater Technol 124:71
18. Goerdeler M, Gottstein G (2001) Mater Sci Eng A 309–310:377
19. Zhilyaev AP, Swaminathan S, Gimazov AA et al (2008) J Mater Sci 43:7451. doi:10.1007/s10853-008-2714-y
20. Ivanisenko Y, Wunderlich RK, Valiev RZ et al (2003) Scr Mater 49:947
21. Valiev RZ, Islamgaliev RK, Alexandrov IV (2000) Prog Mater Sci 45:103
22. Chowdhury SG, Mondal A, Gubicza J et al (2008) Mater Sci Eng 490A:335
23. Mishra A, Kad BK, Gregori F et al (2007) Acta Mater 55:13
24. Shin DH, Park JJ, Kim YS et al (2002) Mater Sci Eng A 328:98
25. Ungár T (2007) J Mater Sci 42:1584. doi:10.1007/s10853-006-0696-1
26. Sivaraman A, Chakkingal U (2008) J Mater Sci 43:7432. doi:10.1007/s10853-008-2871-z
27. Huang JY, Zhu YT, Jiang H et al (2001) Acta Mater 49:1497
28. Xu C, Horita Z, Langdon TG (2008) J Mater Sci 43:7286. doi:10.1007/s10853-008-2624-z
29. Nedjad SH, Meidani H, Ahmadabadi MN (2008) Mater Sci Eng A 475:224
30. Enikeev NA, Kimb HS, Alexandrov IV (2007) Mater Sci Eng A 460–461:619
31. Mulyukov RR, Imayev RM, Nazarov AA (2008) J Mater Sci 43:7257. doi:10.1007/s10853-008-2777-9
32. Xia K, Wu X, Honma T et al (2007) J Mater Sci 42:1551. doi:10.1007/s10853-006-0819-8
33. Sakai G, Horita Z, Langdon TG (2005) Mater Sci Eng A 393:344
34. Kamikawa N, Tsuji N, Minamino Y (2004) Sci Technol Adv Mater 5:163
35. Saito Y, Tsuji N, Utsunomiya H et al (1998) Scr Mater 39:1221
36. Lee JW, Park JJ (2002) J Mater Process Technol 130:208
37. Peng K, Su L, Shaw LL et al (2007) Scr Mater 56:987
38. Toth LS (2005) Comput Mater Sci 32:568
39. Krishnaiah A, Chakkingal U, Venugopal P (2005) Mater Sci Eng A 410:337
40. Les P, Zehetbauer MJ (1994) Key Eng Mater 97:335
41. Zehetbauer MJ (1993) Acta Mater 41:589
42. Zehetbauer MJ, Stuwe HP, Vorhauer A et al (2003) Adv Eng Mater 5:330
43. Mecking H, Kocks U (1981) Acta Mater 29:1865
44. Wildsford DK (1999) Metall Mater Trans A 30:2391
45. Lapovok R, Torre FHD, Sandlin J et al (2005) J Mech Phys Solids 53:729
46. Humphreys FJ, Hatherly M (2004) Recrystallization and related annealing phenomena. Elsevier, Oxford
47. Nes E, Marthinsen K (2002) Mater Sci Eng A 322:176
48. Peczak P (1995) Acta Metall Mater 43:1279
49. Rezvanian O, Zikry MA, Rajendran AM (2006) Mech Mater 38:1159